Journal of Crystal Growth 460 (2017) 134–138

Contents lists available at ScienceDirect

Journal of Crystal Growth

journal homepage: www.elsevier.com/locate/jcrysgro

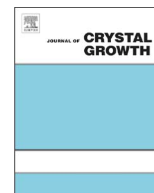

Growth of uniform $CaGe_2$ films by alternating layer molecular beam epitaxy

Jinsong Xu, Jyoti Katoch, Adam S. Ahmed, Igor V. Pinchuk, Justin R. Young, Ezekiel Johnston-Halperin, Jonathan Pelz, Roland K. Kawakami*

Department of Physics, The Ohio State University, Columbus, OH 43210, United States

ARTICLE INFO

Communicated by: K.H. Ploog

Keywords:
A2. Molecular beam epitaxy
A2. Alternating layer epitaxy
B1. Calcium compounds
B1. Nanomaterials

ABSTRACT

Layered Zintl phase van der Waals (vdW) materials are of interest due to their strong spin-orbit coupling and potential for high mobility. Here, we report the successful growth of large area $CaGe_2$ films, as a model of layered Zintl phase materials, on atomically flat Ge(111) substrates by molecular beam epitaxy (MBE) using an alternating layer growth (ALG) protocol. Reflection high energy electron diffraction (RHEED) patterns of the Ge buffer layer and $CaGe_2$ indicate high quality two dimensional surfaces, which is further confirmed by atomic force microscopy (AFM), showing atomically flat and uniform $CaGe_2$ films. The appearance of Laue oscillations in X-ray diffraction (XRD) and Kiessig fringes in the X-ray reflectivity (XRR), which are absent in co-deposited $CaGe_2$, confirms the uniformity of the $CaGe_2$ film and the smoothness of the interface. These results demonstrate a novel method of deposition of $CaGe_2$ that could be also applied to other layered Zintl phase vdW materials. Also, the high quality of the $CaGe_2$ film is promising for the exploration of novel properties of germanane.

1. Introduction

Two dimensional (2D) van der Waals (vdW) materials have emerged as an extremely active field of research, led by the discovery of graphene and its unique properties compared to conventional 3D materials. While the Dirac cone band structure of graphene produces interesting physical phenomena [1–5], the lack of a band gap has proven problematic for transistor and optoelectronic applications. Several methods have been attempted to overcome this drawback and open a gap [6–8], but there has been limited success in producing the large band gaps necessary for practical functionality. These intrinsic limitations of graphene have prompted the rapid development of additional 2D vdW materials with a native band gap and/or strong spin-orbit coupling, such as hexagonal boron nitride [9], silicene [10] and transition metal dichalcogenides [11,12]. Layered Zintl phase materials are another class of 2D vdW material that can be metallic, semiconducting, magnetic, or superconducting [13–16], and are predicted to possess topological states [17,18]. Zintl phases typically comprise of group I (alkali metal) or group II (alkaline earth) cations and group 13–16 anions (post transition metal or metalloid). Some of these materials are exfoliatable due to weak bonding between layers. Very recently, $NaSn_2As_2$ (a member of Zintl phases) was demonstrated to be an air-stable, exfoliatable semimetal [19], which expands the family of exfoliatable 2D vdW materials. Besides novel spin dependent phenomena due to strong spin-orbit coupling inherent to heavy atoms inside these materials, Zintl phases potentially have higher mobility and conductivity compared with transition metals [19]. Furthermore, layered Zintl phases can be transformed into hydrogen- and organic-functionalized graphane analog materials [20–23]. In particular, $CaGe_2$, whose crystal structure is shown in Fig. 1, has generated substantial interest because it can be converted to 2D layered germanane (GeH) by chemical de-intercalation [20], which could ultimately lead to a robust quantum spin Hall effect [24,25]. To date, most of the studies on Zintl phase materials has focused on bulk crystals [26]. Recently, our group has developed a molecular beam epitaxy (MBE) method for growing thin films of $CaGe_2$ by co-depositing elemental Ca and Ge onto a Ge(111) substrate [21,22]. These films are atomically flat locally and exhibit good crystallinity, but also possess macroscopic cracks that are visible under optical microscopy. Therefore, a challenge is to develop new growth procedures for obtaining continuous films without cracks while maintaining good local structure.

In this paper, we report the successful growth of large area, uniform $CaGe_2$ films, as a model of layered Zintl phase materials, by alternating layer growth (ALG) where atomic layers of Ca and Ge are alternately deposited by MBE (also known as migration enhanced epitaxy [27]). In contrast to co-deposited MBE films, the ALG $CaGe_2$ films are free of macroscopic cracks and exhibit thickness oscillations in x-ray diffraction (XRD) and x-ray reflectivity (XRR) scans, indicating uniform films

* Corresponding author.
E-mail address: kawakami.15@osu.edu (R.K. Kawakami).

http://dx.doi.org/10.1016/j.jcrysgro.2016.12.102
Received 14 December 2016; Received in revised form 24 December 2016; Accepted 27 December 2016
Available online 28 December 2016
0022-0248/ © 2017 Elsevier B.V. All rights reserved.

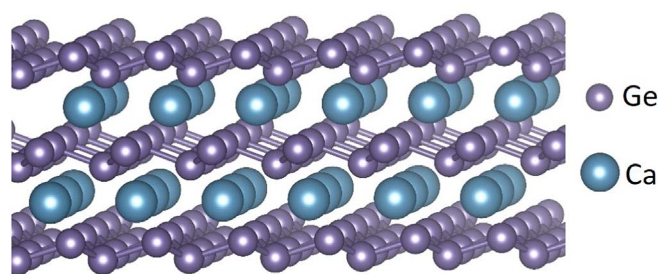

Fig. 1. Schematic of $CaGe_2$ crystal structure.

and interfaces. We find that the growth temperature is a critical parameter for film quality: increasing the temperature from 270 °C to 320 °C improves the reflection high energy electron diffraction (RHEED) patterns and increases the thickness oscillations in the x-ray scans, indicating better crystallinity and improved uniformity. However, if the temperature goes too high (370 °C), the films begin to develop macroscopic cracks. To ensure the accurate timings of the Ca and Ge shutters, modulation of the RHEED intensity oscillation is monitored during growth. In addition, we show that a post-anneal can further improve the quality of $CaGe_2$ films. These results demonstrate a novel method of deposition of $CaGe_2$ that could be also applied to other layered Zintl phase vdW materials. At the same time, these advances in material quality of $CaGe_2$ are also important for the development of high-quality germanane films.

2. Experiment

The $CaGe_2$ films are grown on n-doped Ge(111) substrates (University Wafer) that are cleaned by chemical treatment to remove surface impurities/oxides and to create a protective thin oxide layer [21]. This process involves: (1) sonicating in de-ionized (DI) water for 5 min, (2) etching in a 10:1 mixture of H_2O:NH_4OH for 1 min followed by a 10:1 mixture of H_2O:H_2SO_4 for 1 min to remove surface oxides and metallic impurities, (3) treating in H_2O_2 for 1 min to form a protective thin oxide layer, (4) sonicating in DI water for 5 min to remove surface residues. The Ge(111) substrate is then loaded into the MBE chamber and annealed at 650 °C for 30 min to remove the protective thin oxide layer. Next an atomically flat Ge buffer layer is grown on the Ge(111) substrate before $CaGe_2$ growth by depositing Ge at a rate of 3 Å/min as the substrate is heated from 180 °C to 730 °C at a rate of 5 °C/min. After Ge buffer layer growth, the substrate is cooled down to the growth temperature to start $CaGe_2$ alternating layer growth by opening and closing Ca and Ge cell shutters alternatively to deliver alternating monolayer doses of Ca or Ge. Elemental Ca (99.99%, Sigma Aldrich) and Ge (99.9999%, Alfa Aesar) are evaporated from effusion cells. Typical growth rates are several Å/min as measured using a quartz crystal microbalance. Throughout the entire growth process, *in situ* RHEED is used to monitor the sample surface which is critical for ALG. Surface morphology is examined *ex situ* by atomic force microscopy (AFM) while the crystal structure is probed by XRD and XRR. Since $CaGe_2$ is very sensitive to air, all $CaGe_2$ samples characterized by AFM, XRD and XRR are capped with 20 nm of Ge grown at room temperature.

3. Results and discussion

3.1. Growth temperature

The substrate temperature during deposition is a critical parameter for obtaining high quality $CaGe_2$ films with the ALG method. Fig. 2 presents both RHEED and AFM images of the Ge buffer layer and $CaGe_2$ films grown at three different substrate temperatures. The RHEED pattern of the Ge buffer layer (Fig. 2(a)) shows an extremely clear 2×8 reconstruction of a clean Ge(111) surface, and the AFM image shows atomically flat terraces and an overall RMS roughness of 1.88 nm over the entire image. Fig. 2(b-d) show the RHEED and AFM data from 10 nm $CaGe_2$ films grown by the ALG method at three different growth temperatures (T_{growth}) of 270 °C, 320 °C, and 370 °C. Because Ca re-evaporation occurs above ~500 °C [21], this is not a significant factor for these growth temperatures. Fig. 3 shows the corresponding XRD and XRR scans for these samples.

Beginning with the sample grown at 270 °C, the RHEED pattern exhibits the characteristic 3× reconstruction peak of $CaGe_2$ (Fig. 2(b)) and the XRD has a peak at θ=17.39° which corresponds to a $CaGe_2$ *c*-axis lattice parameter of 5.094 Å (Fig. 3(a)). In addition, the AFM image shows similar topography to the Ge buffer layer (RMS roughness

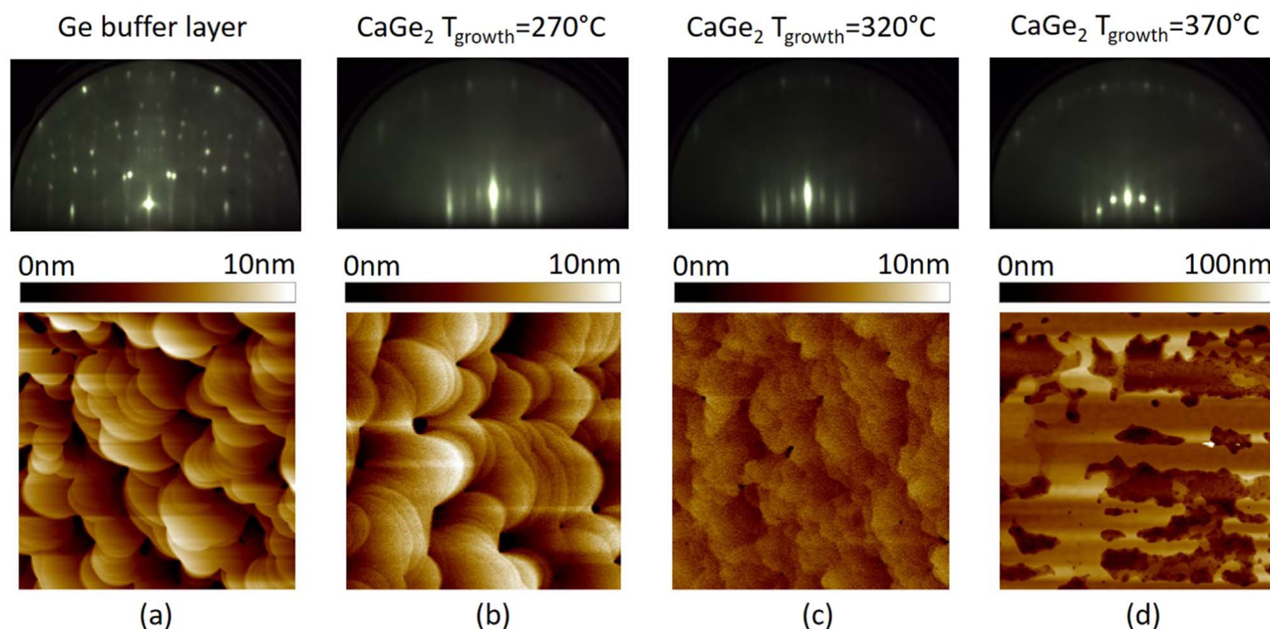

Fig. 2. $CaGe_2$ growth as a function of temperature. Films are characterized by *in situ* RHEED (top row) and *ex situ* AFM (bottom row) images. AFM scan areas are 10 μm×10 μm. (a) Ge buffer layer images before $CaGe_2$ growth. The next three images are 10 nm $CaGe_2$ grown at (b) 270 °C (c) 320 °C (d) 370 °C. For the AFM images, the $CaGe_2$ films are capped with 20 nm Ge grown at room temperature.

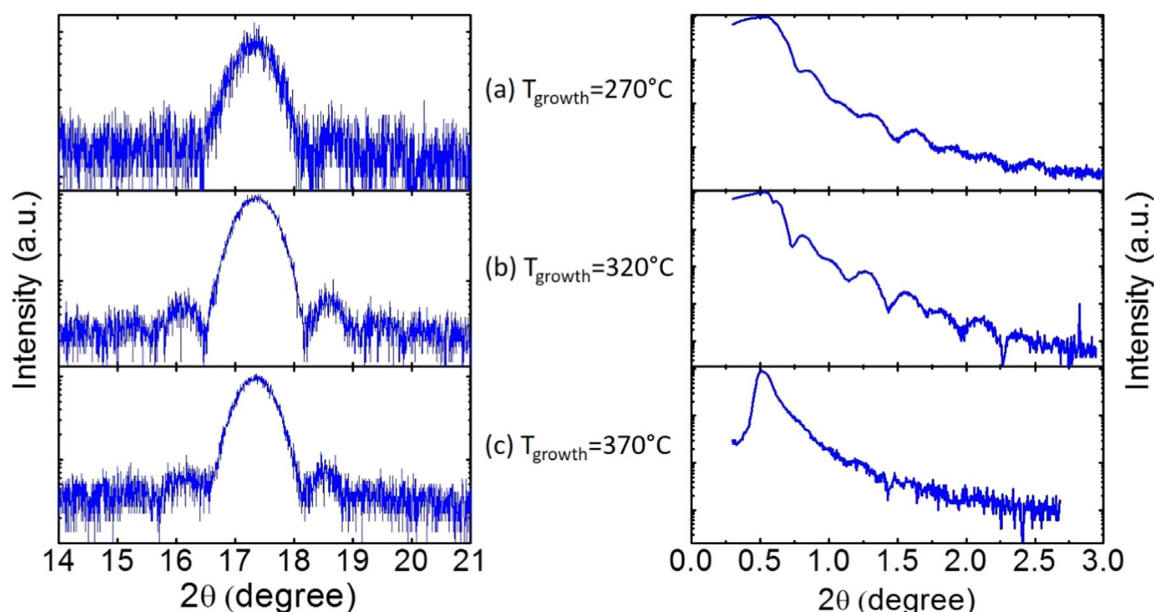

Fig. 3. $CaGe_2$ growth as a function of temperature. Films are characterized by XRD (left column) and XRR reflectivity (right column). The three images are 10 nm $CaGe_2$ grown at (a) 270 °C (b) 320 °C (c) 370 °C. Samples are capped with 20 nm of Ge at room temperature.

of 1.87 nm), indicating that the $CaGe_2$ growth is uniform, smooth, and free of cracks. This is further confirmed by the appearance of Kiessig fringes in XRR (Fig. 3(a)).

Increasing the growth temperature to 320 °C produces improvements to the material quality. Compared to $CaGe_2$ grown at 270 °C, the films grown at 320 °C have sharper RHEED patterns (Fig. 2(c)) and clear Laue oscillations in XRD (Fig. 3(b)), indicating that the $CaGe_2$ film has flatter and more uniform surfaces and interfaces. In addition, the $CaGe_2$ film exhibits better uniformity (RMS roughness of 0.70 nm) and crack-free structure as shown by AFM (Fig. 2(c)). The slightly stronger Kiessig fringes in XRR also demonstrate good uniformity of the film and interfaces (Fig. 3(b)).

Further increases in growth temperature, however, lead to the formation of cracks within the film, which is evident in the rough morphology (RMS roughness of 11.5 nm) observed in AFM of films grown at 370 °C (Fig. 2d). This is consistent with the weaker Laue oscillations in the XRD and the disappearance of Kiessig fringes in XRR (Fig. 3(c)). On the other hand, the RHEED patterns are better for 370 °C growth, exhibiting 2D-like spots, because adatoms have higher mobility and can form flatter surfaces within small (μm-sized) regions. Nevertheless, the presence of cracks and a rough morphology are unfavorable for future device applications.

It is also worthwhile to consider the layer-by-layer evolution of the RHEED pattern for growth at 320 °C, as shown in Fig. 4. Notably, the

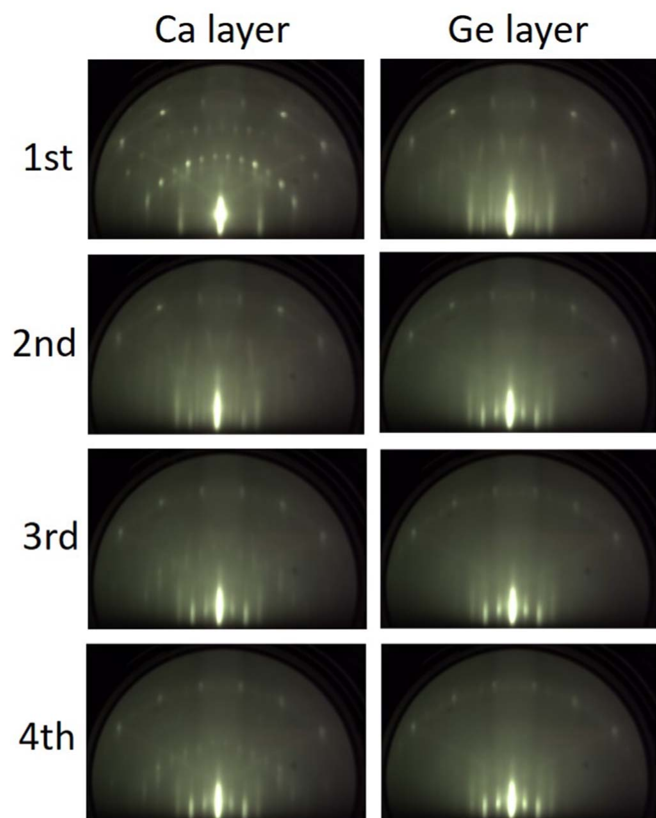

Fig. 4. Evolution of the RHEED pattern for the initial Ca and Ge layers grown at 320 °C.

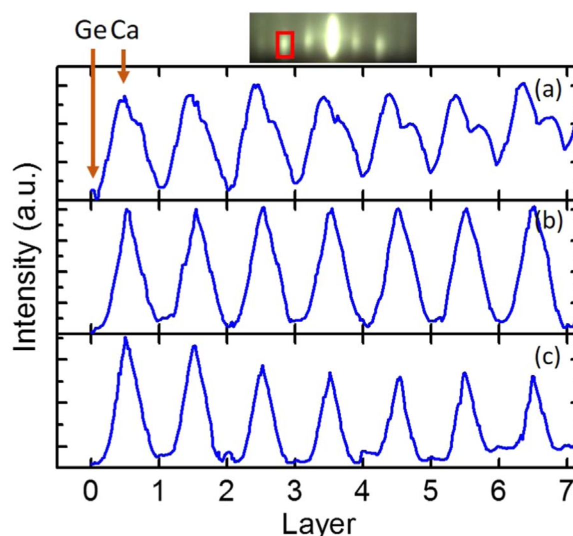

Fig. 5. Modulation of RHEED intensity (monitored at the peak outlined in red box) for different Ca layer thickness. The Ge layer thickness is fixed at 1 monolayer for each growth layer, while the Ca layer thickness varies: (a) 0.93 monolayer (b) 1 monolayer and (c) 1.07 monolayer for each growth layer. (For interpretation of the references to color in this figure legend, the reader is referred to the web version of this article.)

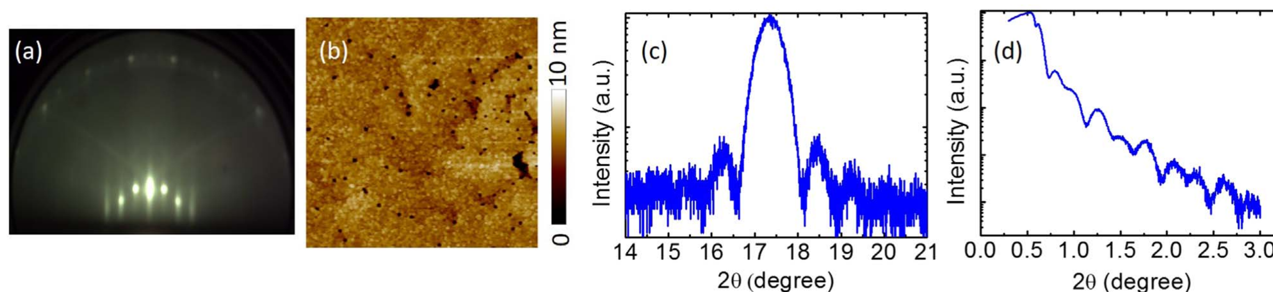

Fig. 6. Characterization of 10 nm $CaGe_2$ films with post-anneal (a) RHEED (b) AFM (c) XRD (d) XRR.

RHEED pattern after the first layer of Ca deposition is substantially different from the Ge substrate (Fig. 2a). Subsequently, the RHEED pattern gradually evolves for the first three cycles of Ca and Ge layer deposition and reaches a stable 3x reconstruction pattern that reproduces for subsequent cycles. This is in stark contrast to what occurs in the high temperature co-deposition growth of $CaGe_2$ [21], where the RHEED pattern obtains the 3x reconstruction after a few seconds of exposure to Ca flux (while a typical monolayer deposition takes 30–60 s). This indicates that there is substantial interaction of Ca with the Ge substrate for the high temperature co-deposition growth method. In contrast, the steady layer-by-layer evolution of the RHEED pattern shows a more controlled formation of the interface in the ALG method.

3.2. Growth timing

To achieve high quality $CaGe_2$ films using the ALG method, it is important to get correct dose for each atomic layer. For this purpose, we monitor the modulation of RHEED intensity oscillations to optimize the timing for the opening and closing of the Ca and Ge shutters [28,29]. When complete monolayers are deposited, the amplitude of RHEED oscillations is constant. However, if one of the shutters is mistimed then the amplitude of RHEED oscillations is modulated with a slowly varying envelope. This is best illustrated in Fig. 5, which shows a series of RHEED intensity modulations for three different timings of the Ca deposition. For these growths, we use the optimized growth temperature of 320 °C. When the Ge shutter is opened and Ge is deposited, the RHEED intensity (measured in the red box in the RHEED pattern of Fig. 5) starts increasing with the RHEED beam incident along the Ge $[11\bar{2}0]$ azimuth. When the Ca shutter is open and Ca is deposited, the RHEED intensity starts decreasing. The intensity achieves a maximum value following the deposition of a full monolayer Ge and a minimum value following the deposition of a full monolayer Ca. The Ge dose is kept at 1 full monolayer for the three different growths shown in Fig. 5, while the Ca dose is varied by adjusting the shutter timing: (a) 0.93 monolayer; (b) 1 monolayer and (c) 1.07 monolayer. For a full monolayer deposition of Ca (Fig. 5(b)), both the intensity maximum and minimum will remain constant after several layers deposition of $CaGe_2$. On the other hand, mistimed Ca deposition will produce modulations of the RHEED intensity oscillations, which is a typical characteristic of mistimed atomic layer MBE growth [28,29]. For an insufficient dose of Ca (Fig. 5(a)), the intensity minimum will increase with each succeeding layer of deposition and a shoulder peak appears. For an excess dose of Ca (Fig. 5(c)), the intensity maximum will decrease. Thus, by monitoring the RHEED intensity during growth, the correct dosing of Ge and Ca can be ensured.

3.3. Post-anneal

After optimizing the growth temperature and timing, the AFM, XRD, and XRR characterizations exhibit optimal values. However, the RHEED pattern is not optimized; the 370 °C growth showed the clearest RHEED patterns, indicating flatter terraces despite the presence of macroscopic cracks. The question becomes whether it is possible to improve the RHEED pattern while maintaining the high quality of the AFM, XRD, and XRR. To determine this, we perform a post-annealing study. Increasing the temperature leads to no apparent changes to the RHEED pattern until ~730 °C, when the pattern begins to sharpen. Therefore, we post-annealed the $CaGe_2$ film at 730 °C for 10 min. As shown in Fig. 6(a), the RHEED pattern is sharper and there are Kikuchi lines appearing, indicating long range order. We do not believe the sharpening of the pattern is primarily due to re-evaporation of excess Ca because such effects should start of occur at ~500 °C [21], and we do not observe any changes near this temperature. Comparing all the characterizations (RHEED, AFM, XRD, XRR) for a 10 nm $CaGe_2$ film without post-anneal (Figs. 2(c) and 3(b)) and with post-anneal (Fig. 6), we find that the post-anneal produces no degradation of the AFM, XRD, and XRR characteristics while the RHEED pattern has improved.

4. Conclusions

We have demonstrated the successful growth of large-area, uniform and crack-free $CaGe_2$ films by the ALG MBE method. By combining RHEED, AFM, XRD and XRR characterizations, we show that the appropriate temperature for high-quality $CaGe_2$ growth is 320 °C. Furthermore, RHEED intensity modulation is used to ensure accurate doses of Ca and Ge. By post-annealing, the $CaGe_2$ film quality is further improved as indicated by sharper RHEED patterns and the appearance of Kikuchi lines. These results demonstrate a novel method of deposition of $CaGe_2$ that could be applied to other layered Zintl phase materials. Furthermore, the high quality of the $CaGe_2$ films are promising for future studies of germanane.

Acknowledgments

We acknowledge the support of NSF MRSEC (DMR-1420451).

References

[1] K.S. Novoselov, A.K. Geim, S.V. Morozov, D. Jiang, M.I. Katsnelson, I.V. Grigorieva, S.V. Dubonos, A.A. Firsov, Nature 438 (2005) 197.
[2] Y. Zhang, Y.W. Tan, H.L. Stormer, P. Kim, Nature 438 (2005) 201.
[3] V.P. Gusynin, S.G. Sharapov, Phys. Rev. Lett. 95 (2005) 146801.
[4] A.K. Geim, K.S. Novoselov, Nat. Mater. 6 (2007) 183.
[5] Y. Wang, D. Wong, A.V. Shytov, V.W. Brar, S. Choi, Q. Wu, H.-Z. Tsai, W. Regan, A. Zettl, R.K. Kawakami, S.G. Louie, L.S. Levitov, M.F. Crommie, Science 340 (2013) 734.
[6] K. Nakada, M. Fujita, G. Dresselhaus, M.S. Dresselhaus, Phys. Rev. B 54 (1996) 17954.
[7] T. Ohta, A. Bostwick, T. Seyller, K. Horn, E. Rotenberg, Science 313 (2006) 951.
[8] R. Balog, B. Jorgensen, L. Nilsson, M. Andersen, E. Rienks, M. Bianchi, M. Fanetti, E. Laegsgaard, A. Baraldi, S. Lizzit, Z. Sljivancanin, F. Besenbacher, B. Hammer, T.G. Pedersen, P. Hofmann, L. Hornekaer, Nat. Mater. 9 (2010) 315.
[9] K. Watanabe, T. Taniguchi, H. Kanda, Nat. Mater. 3 (2004) 404.
[10] P. Vogt, P. De Padova, C. Quaresima, J. Avila, E. Frantzeskakis, M.C. Asensio, A. Resta, B. Ealet, G. Le Lay, Phys. Rev. Lett. 108 (2012) 155501.
[11] K.F. Mak, C. Lee, J. Hone, J. Shan, T.F. Heinz, Phys. Rev. Lett. 105 (2010) 136805.
[12] A. Splendiani, L. Sun, Y. Zhang, T. Li, J. Kim, C.Y. Chim, G. Galli, F. Wang, Nano Lett. 10 (2010) 1271.
[13] J.F. Morar, M. Wittmer, Phys. Rev. B 37 (1988) 2618.
[14] M.J. Evans, Y. Wu, V.F. Kranak, N. Newman, A. Reller, F.J. Garcia-Garcia,

U. Häussermann, Phys. Rev. B 80 (2009) 064514.
[15] M.J. Evans, M.H. Lee, G.P. Holland, L.L. Daemen, O.F. Sankey, U. Häussermann, J. Solid State Chem. 182 (2009) 2068.
[16] E. Noguchi, K. Sugawara, R. Yaokawa, T. Hitosugi, H. Nakano, T. Takahashi, Adv. Mater. 27 (2015) 856.
[17] Q.D. Gibson, L.M. Schoop, L. Muechler, L.S. Xie, M. Hirschberger, N.P. Ong, R. Car, R.J. Cava, Phys. Rev. B 91 (2015) 205128.
[18] H. Huang, J. Liu, D. Vanderbilt, W. Duan, Phys. Rev. B 93 (2016) 201114 (R).
[19] M.Q. Arguilla, J. Katoch, K. Krymowski, N.D. Cultrara, J. Xu, X. Xi, A. Hanks, S. Jiang, R.D. Ross, R.J. Koch, S. Ulstrup, A. Bostwick, C.M. Jozwiak, D.W. McComb, E. Rotenberg, J. Shan, W. Windl, R.K. Kawakami, J.E. Goldberger, ACS Nano 10 (2016) 9500.
[20] E. Bianco, S. Butler, S. Jiang, O.D. Restrepo, W. Windl, J.E. Goldberger, ACS Nano 7 (2013) 4414.
[21] I.V. Pinchuk, P.M. Odenthal, A.S. Ahmed, W. Amamou, J.E. Goldberger, R.K. Kawakami, J. Mater. Res. 29 (2014) 410.
[22] W. Amamou, P.M. Odenthal, E.J. Bushong, D.J. O'Hara, Y.K. Luo, J. van Baren, I. Pinchuk, Y. Wu, A.S. Ahmed, J. Katoch, M.W. Bockrath, H.W.K. Tom, J.E. Goldberger, R.K. Kawakami, 2D Mater. 2 (2015) 035012.
[23] S. Jiang, S. Butler, E. Bianco, O.D. Restrepo, W. Windl, J.E. Goldberger, Nat. Commun. 5 (2014) 3389.
[24] C. Si, J. Liu, Y. Xu, J. Wu, B.-L. Gu, W. Duan, Phys. Rev. B 89 (2014) 115429.
[25] R.-W. Zhang, W.-X. Ji, C.-W. Zhang, S.-S. Li, P. Li, P.-J. Wang, J. Mater. Chem. C 4 (2016) 2088.
[26] T.F. Fässler, Zintl Phases: Principles and Recent Developments, Springer-Verlag, Berlin, Heidelberg, 2011.
[27] Y. Horikoshi, Semicond. Sci. Technol. 8 (1993) 1032.
[28] J.H. Haeni, C.D. Theis, D.G. Schlom, J. Electroceram. 4 (2000) 385.
[29] Y. Horikoshi, M. Kawashima, H. Yamaguchi, Jpn J. Appl. Phys. 25 (1986) L868.